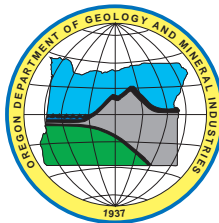


State of Oregon
Department of Geology and Mineral Industries
Vicki S. McConnell, State Geologist

Open-File Report O-08-09

**REGIONAL LANDSLIDE HAZARD MAPS OF THE
SOUTHWEST QUARTER OF THE BEAVERTON QUADRANGLE,
WEST BULL MOUNTAIN PLANNING AREA,
WASHINGTON COUNTY, OREGON**

By
William J. Burns¹



2008

¹Oregon Department of Geology and Mineral Industries, 800 NE Oregon Street #28, Suite 965, Portland, Oregon 97232

NOTICE

The Oregon Department of Geology and Mineral Industries is publishing this map because the subject matter is consistent with the mission of the Department. The map is not intended to be used for site-specific planning. It may be used as a general guide for emergency response planning. Maps in this publication depict landslide hazard areas on the basis of limited data as described further in the text. The maps cannot serve as a substitute for site-specific investigations by qualified practitioners. Site-specific data may give results that differ from those shown on the maps.

Oregon Department of Geology and Mineral Industries O-08-09
Published in conformance with ORS 516.030

For copies of this publication or other information about Oregon's geology and natural resources, contact:

Nature of the Northwest Information Center
800 NE Oregon Street #5, Suite 177
Portland, Oregon 97232
(503) 872-2750
<http://www.naturenw.org>

or these DOGAMI field offices:

Baker City Field Office
1510 Campbell Street
Baker City, OR 97814-3442
Telephone (541) 523-3133
Fax (541) 523-5992

Grants Pass Field Office
5375 Monument Drive
Grants Pass, OR 97526
Telephone (541) 476-2496
Fax (541) 474-3158

For additional information:
Administrative Offices
800 NE Oregon Street #28, Suite 965
Portland, OR 97232
Telephone (971) 673-1555
Fax (971) 673-1562
<http://www.oregongeology.com>
<http://egov.oregon.gov/DOGAMI/>

TABLE OF CONTENTS

1.0 EXECUTIVE SUMMARY	1
2.0 SIGNIFICANCE OF THE PROBLEM	2
3.0 PURPOSE AND SCOPE	2
4.0 CREATION OF THE HAZARD MAPS	2
4.1 Lidar-based landslide inventory	2
4.2 Shallow-seated landslide susceptibility	5
4.3 Deep-seated landslide susceptibility	13
5.0 RESULTS AND DISCUSSION	14
6.0 RECOMMENDATIONS	17
7.0 ACKNOWLEDGEMENTS	17
8.0 REFERENCES	17

LIST OF FIGURES

Figure 1. Location of West Bull Mountain Planning Area	1
Figure 2. Map of previous identified landslides and map of potential debris flow hazard areas	3
Figure 3. Diagram and equation for calculation of estimated depth to failure	5
Figure 4. Landslide inventory map of the southwest quarter of the Beaverton quadrangle, Washington County, Oregon.	6
Figure 5. Infinite slope analysis: diagram, parameters, and equation	7
Figure 6. Geologic-material properties map	8
Figure 7. Slope map created from lidar-derived digital elevation model	9
Figure 8. Diagram of the 2 horizontal to 1 vertical ratio used to create the buffers	9
Figure 9. Diagram of the 2H:1V head scarp buffer	11
Figure 10. Diagram of the 2H:1V buffer applied to all factor of safety less than 1.5	11
Figure 11. Shallow-seated landslide susceptibility map of the southwest quarter of the Beaverton quadrangle, Washington County, Oregon	12
Figure 12. Head scarp retrogression buffer	13
Figure 13. Head scarp buffer	13
Figure 14. Generalized geologic map overlain with slopes greater than 10 degrees and identified deep-seated landslides	14
Figure 15. Deep-seated landslide susceptibility map of the southwest quarter of the Beaverton quadrangle, Washington County, Oregon	16

LIST OF TABLES

Table 1. Tabular data fields used for lidar-based landslide inventory	4
Table 2. Conservative typical soil and rock material properties	8
Table 3. Final hazard zone matrix for shallow-seated landslides	10
Table 4. Final hazard zone matrix for deep-seated landslides	15

LIST OF PLATES

Plate 1. Landslide inventory map of the southwest quarter of the Beaverton quadrangle, Washington County, Oregon
Plate 2. Shallow-seated landslide susceptibility map of the southwest quarter of the Beaverton quadrangle, Washington County, Oregon
Plate 3. Deep-seated landslide susceptibility map of the southwest quarter of the Beaverton quadrangle, Washington County, Oregon

1.0 EXECUTIVE SUMMARY

On October 1, 2007, the Oregon Department of Geology and Mineral Industries (DOGAMI) entered an inter-governmental agreement with Washington County, Oregon (project no. 100075, purchase order 141319) to perform regional landslide hazard evaluation of the West Bull Mountain Planning Area (WBMPA) as shown in Figure 1.

Deliverables of this study include the following:

- this report text
- hazard maps:
 - lidar-based landslide inventory map (Figure 4; Plate 1)
 - shallow-seated landslide susceptibility map (Figure 11; Plate 2)
 - deep-seated landslide susceptibility map (Figure 15; Plate 3)
- geographic information system (GIS) files:
 - landslide inventory
 - shallow-seated susceptibility
 - deep-seated susceptibility

A lidar-based landslide inventory mapping protocol (Burns and Madin, 2008) was used to create a landslide inventory of the southwest quarter of the Beaverton, Oregon, U.S. Geological Survey topographic quadrangle. Ninety-eight landslide deposits were located. Forty-seven of these are within the WBMPA. Eighty-three of these were classified as shallow, nine as deep, and six as debris flow deposits. The average prefailure slope angle is 28 degrees. The average landslide area is roughly 20,000 ft² (1850 m²), which is approximately the size of a football field. The average depth of failure for the shallow-seated landslides is 8.5 ft (2.6 m), and the average depth of failure for the deep-seated landslides is 26 ft (7.9 m).

A lidar-based shallow-seated landslide susceptibility mapping protocol (Burns, 2008a) was used to create a shallow-seated landslide susceptibility map of the southwest quarter of the Beaverton quadrangle. The area of the southwest quarter of the quadrangle is roughly 13 mi² (37 km²); 2.0 mi² (5.2 km²) of the total are classified as highly susceptible to shallow-seated landslides, 6.5 mi² (16.3 km²) as moderately susceptible to shallow-seated landslides, and 4.7 mi² (12.2 km²) as less susceptible to shallow-seated landslides.

The lidar-based deep-seated landslide susceptibility mapping protocol (Burns, 2008b) was used to create a

deep-seated susceptibility map of the southwest quarter of the Beaverton quadrangle.

The landslide inventory map, shallow-seated susceptibility map, and deep-seated susceptibility map were developed with input from many sources and expertise gained from years of experience; however, several limitations underscore that these maps are designed for regional applications and should not be used as an alternative to site-specific studies in critical areas. These limitations are described in detail on Plates 1–3.

These maps are intended to provide users with basic information regarding landslides and the susceptibility to landslides within the mapped area. These maps contain useful information to guide site-specific investigations for future development, to assist in regional planning and development, to mitigate existing landslides and slopes, and to prepare for emergency situations, such as storm events and earthquakes. While we reiterate that these data are not appropriate for site-specific evaluations, the data are valuable for regional screening for landslides and selection of appropriate areas on which to focus further site-specific studies. The data are particularly suitable for incorporation and con-

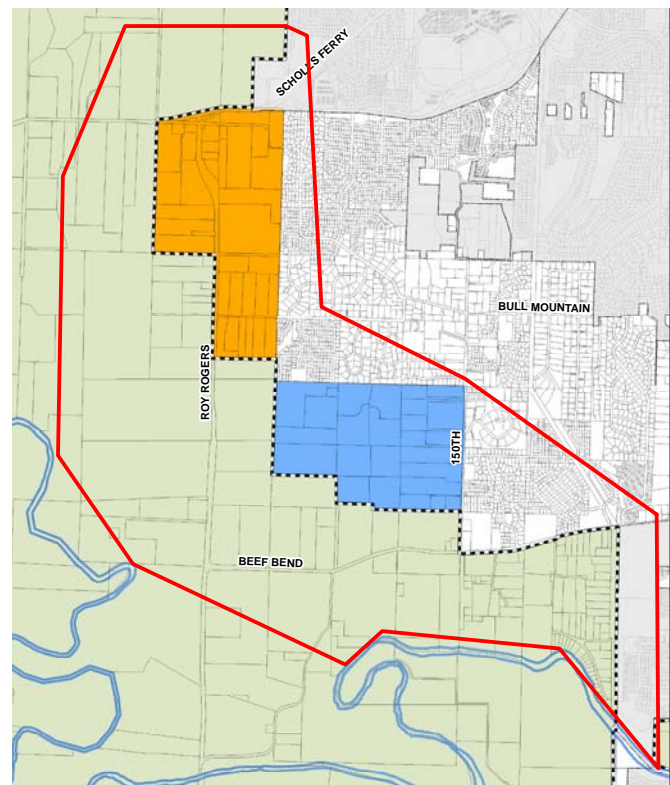


Figure 1. West Bull Mountain Planning Area, Washington County, Oregon (outlined in red; approximately 3.5 square miles).

sideration into regional GIS databases for a multitude of purposes. These include but are not limited to city and county hillside development ordinances, issuance of building permit conditions, public works planning and operations, and environmental and sustainability issues.

2.0 SIGNIFICANCE OF THE PROBLEM

Landslides are one of the most widespread and damaging natural hazards in Oregon. In order to begin reducing losses from landslides (mitigation), areas of landslide hazard must first be located. The first step in landslide hazard identification is to create an inventory of past (historic and prehistoric) landslides. The inventory can then be used to create susceptibility maps that display areas at risk for landslides.

3.0 PURPOSE AND SCOPE

The purpose of this study is to evaluate the regional relative landslide hazard and to provide recommendations to Washington County. Seismic, civil, and environmental evaluation of any kind are beyond the scope of this project.

We performed our services in accordance with the intergovernmental agreement with Washington County (project no. 100075, purchase order 141319). DOGAMI is not responsible for independent conclusions, opinions, or recommendations made by others based on information provided in this report.

Considering the dynamic environment in Oregon, the inherent risks associated with development in hilly areas, and the fact that the study of all geologic hazard processes is not completely known to the professional and research community at this time, we warn that our report does not assure any safety or warranty from geologic hazards. The maps in this study were developed with input from many sources and expertise gained from years of experience; however, several limitations underscore that these maps are designed for regional applications and should not be used as an alternative to site-specific studies. These limitations are described in detail in Plates 1–3.

4.0 CREATION OF THE HAZARD MAPS

As part of this study, we created three landslide hazard maps: 1) lidar-based landslide inventory, 2) shallow-seated landslide susceptibility, and 3) deep-seated landslide susceptibility. The methods employed to create these maps are described below.

4.1 Lidar-based landslide inventory

Recently, very high resolution, high-accuracy digital elevation models (DEM) developed using light detection and ranging (lidar) data have become available for some parts of Oregon. These new data give us a much better image of the surface geomorphology, allowing identification of features associated with landslides, such as concave slope depressions, vertical or steep scarps, shear zones located along the flanks of a landslide, and shortening features of landslides such as toes, transverse ridges, and snouts (Burns, 1999). Recognition of such features can be used to identify landslides with a high level of certainty and map them accurately. In the past, most accurate, higher-certainty, landslide maps were created using a combination of aerial photography and extensive field survey. The use of lidar derived bare earth digital elevation model (DEM) is the key to the landslide mapping performed in this study.

Prior to beginning lidar-based mapping of landslides in the WBMPA, we reviewed two landslide inventories: 1) the 1996-1997 storm events inventory (DOGAMI Special Paper 34 [Hofmeister, 2000]) and the Statewide Landslide Information Database for Oregon (SLIDO) (Burns, and others, 2008). The latest geologic maps of the area, DOGAMI Open-File Report O-04-02 and DOGAMI Open-File Report O-90-02 (Madin, 2004; Madin, 1990), were also reviewed. No landslides from any of these sources were identified within the WBMPA (Figure 2). We also reviewed DOGAMI Interpretive Map Series 22 (IMS-22) (Figure 2) (Hofmeister and others, 2002). Again, no potential hazard was identified within the WBMPA.

After review of previous regional landslide hazard studies, we mapped the entire southwestern quarter of the U.S. Geological Survey 7.5' Beaverton topographic quadrangle (which encompasses the WBMPA) using lidar-derived DEM and DEM derivatives including shaded relief (hillshades), slope maps, and topographic

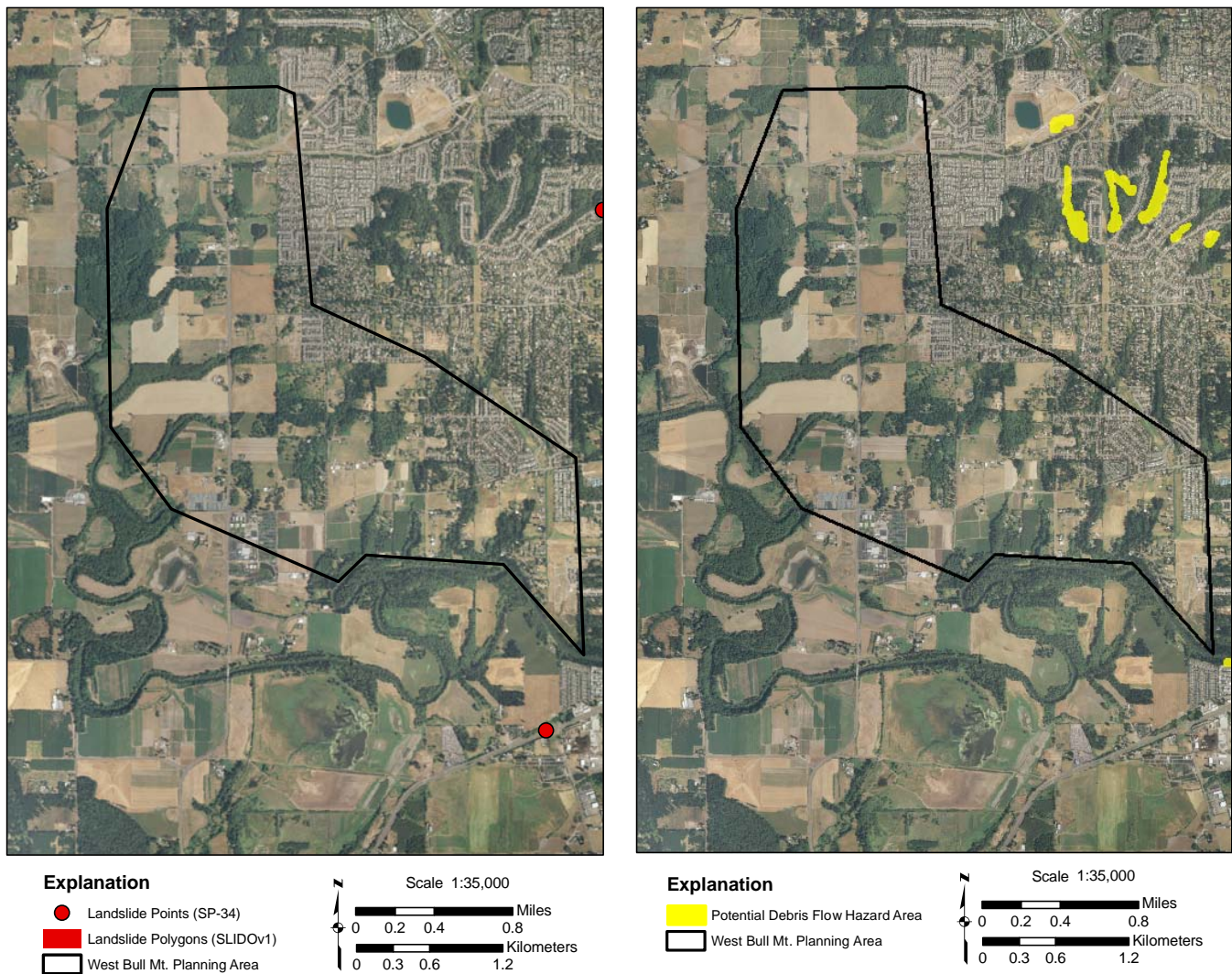


Figure 2. (left) Map of previous identified landslides from DOGAMI publications O-04-02 (Madin, 2004), SP-34 (Hofmeister, 2000), and SLIDO-1 (Burns and others, 2008), and (right) map of potential debris flow hazard areas from DOGAMI IMS-22 (Hofmeister and others, 2002). Note that no landslide points (SP-34), landslide polygons (SLIDO-1), or potential debris flow hazard areas (IMS-22) were identified within the WBMPA (black outline).

contours. In addition to the lidar-derived images, we used an orthophoto of similar age to the lidar data to help differentiate between some man-made and natural landforms. We identified landslides solely from ground surface morphology. Morphologic features include head scarps, hummocky topography, convex and concave slope areas, offset drainages, flank shear offsets, and internal scarps. We created the inventory following the protocol defined by Burns and Madin (2008).

Because landslides and landslide features are not all the same size, we mapped at several different scales, in this order:

- 1:24,000 scale (the native scale of a standard printed 7.5 minute topographic quadrangle)
- 1:10,000
- 1:4,000

Spatial data and tabular data were mapped into a GIS. Spatial data include the following four elements:

- polygon (outline) of the mapped landslide deposit
- polygon (outline) of the landslide head scarp
- line of the uppermost extent of the head scarp
- lines of internal scarps

However, all four of these features may not have been present or determinable at every landslide.

Kinds of tabular data collected are shown in Table 1. Some of these tabular data may not have been present or determinable at every landslide. Some items are described in more detail on Plate 1.

One important tabular datum in the landslide inventory is the estimated depth of failure, which was calculated for each identified landslide as shown in Figure 3 (Burns and others, 1998; Burns, 1999; Burns and Madin, 2008).

Using estimated failure depth, we classified each landslide as deep or shallow seated. This differentia-

tion is necessary because different models are used to calculate or estimate regional stability or susceptibility for different depths and for different types of landslides. There is no widely accepted value of division between deep and shallow landslides, so we based our value on the combination of several factors and several other studies (Sidle and Ochiai, 2006; Burns, 1999; Harp and others, 2006). We selected a division value of 15 ft (4.5 m) between shallow- and deep-seated landsliding.

After lidar-derived DEM mapping and tabular database entry were completed, we performed ground

Table 1. Tabular data fields used for lidar-based landslide inventory.

Field Name	Abbreviated Code	Brief Description
Identification	ID	numeric string
Quadrangle name	QUADNAME	7.5 minute quadrangle name
Unique identification	UNIQUE_ID	"QUADNAME"_"ID"
Mapper name	MAPPER_NAM	name of mapper
Type of movement	Type_Move	type of movement
Movement classification	MOVE_CLASS	classification name
Movement classification code	MOVE_CODE	classification code
Confidence of interpretation	CONFIDENCE	confidence of identification
Estimated age	AGE	estimated age
Date of last movement	DATE_MOVE	date of last known movement
Landslide name	NAME	landslide name
Geology	Geol	geologic unit
Adjacent slope	SLOPE	adjacent slope angle
Head scarp height	HSHEIGHT	change in elevation from bottom to top of head scarp or change in elevation from top to toe of fan
Failure depth	FAIL_DEPTH	estimated failure depth
Fan depth	Fan_DEPTH	estimated depth of fan
Deep-shallow	DEEP_SHAL	deep or shallow seated
Horizontal distance HS to IS1	HS_IS1	horizontal distance from head scarp to internal scarp no.1
Horizontal distance IS1 to IS2	IS1_IS2	horizontal distance from internal scarp 1 to internal scarp 2
Horizontal distance IS2 to IS3	IS2_IS3	horizontal distance from internal scarp 2 to internal scarp 3
Horizontal distance IS3 to IS4	IS3_IS4	horizontal distance from internal scarp 3 to internal scarp 4
Average horizontal distance between internal scarps	HDAVE	average horizontal distance between internal scarps
Size of landslide deposit	AREA	size of landslide deposit
Volume of landslide deposit	VOL	volume of landslide deposit

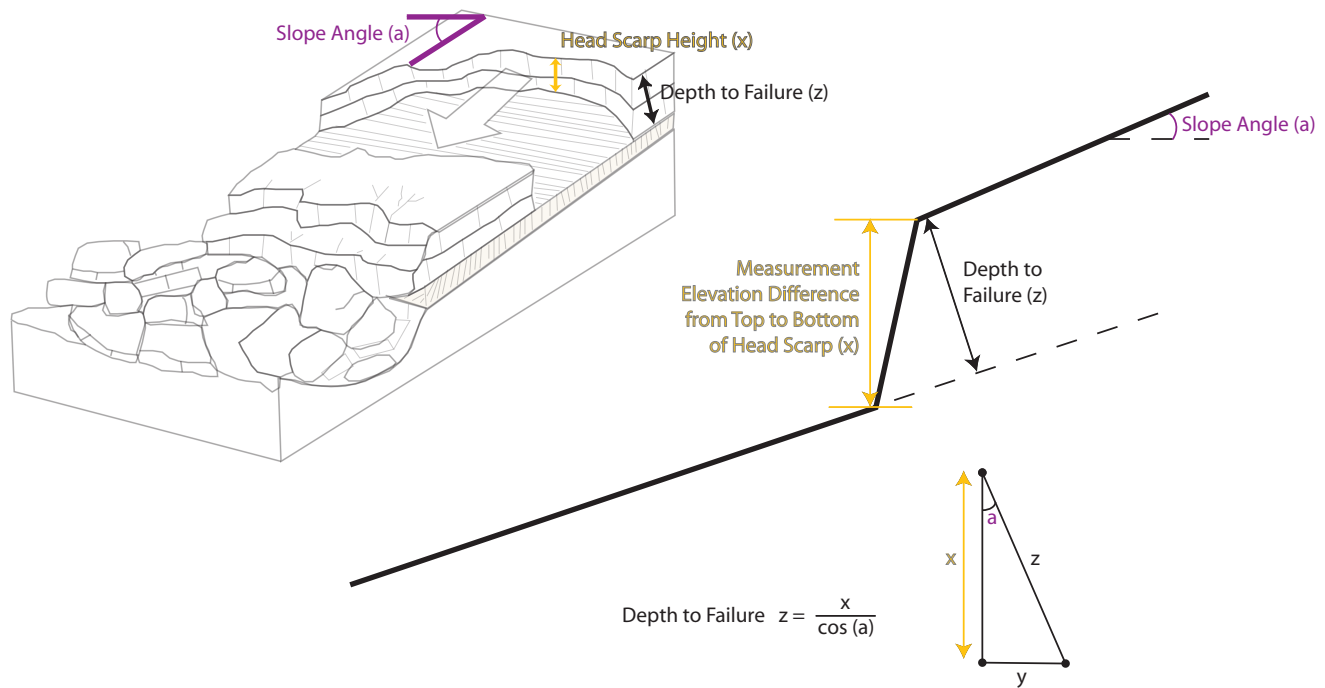


Figure 3. Diagram and equation for calculation of estimated depth to failure.

reconnaissance to field verify the suspected landslide features. Observations made during the reconnaissance were used to revise the lidar-based landslide inventory map, as appropriate.

To assist visualization, we created a 1:8,000-scale map (Plate 1; facsimile in Figure 4) that displays lidar-based landslide inventory data (Beaverton_SWLSdeposits.*, Beaverton_SWLSheadscarps.*, and Beaverton_SWLScarps.*; these GIS files are provided as part of this publication). This map cannot serve as a substitute for site-specific investigations by qualified practitioners. Site-specific data may give results that differ from those shown on this map. Several other limitations are listed on Plate 1.

4.2 Shallow-seated landslide susceptibility

With the lidar-based landslide inventory and several other data sets, we created a shallow-seated (less than 15 ft [4.5 m]) susceptibility map using four main components (Burns, 2008a):

- shallow-seated landslide inventory
- calculation of regional factor of safety (FOS)
- buffers
- combination of the previous three factors into final susceptibility hazard zones

All shallow-seated slides, flows, and spreads were queried out of the lidar-based landslide inventory database and saved to a separate GIS file.

To calculate the factor of safety (FOS) for shallow-seated landsliding, we used the infinite slope equation shown in Figure 5.

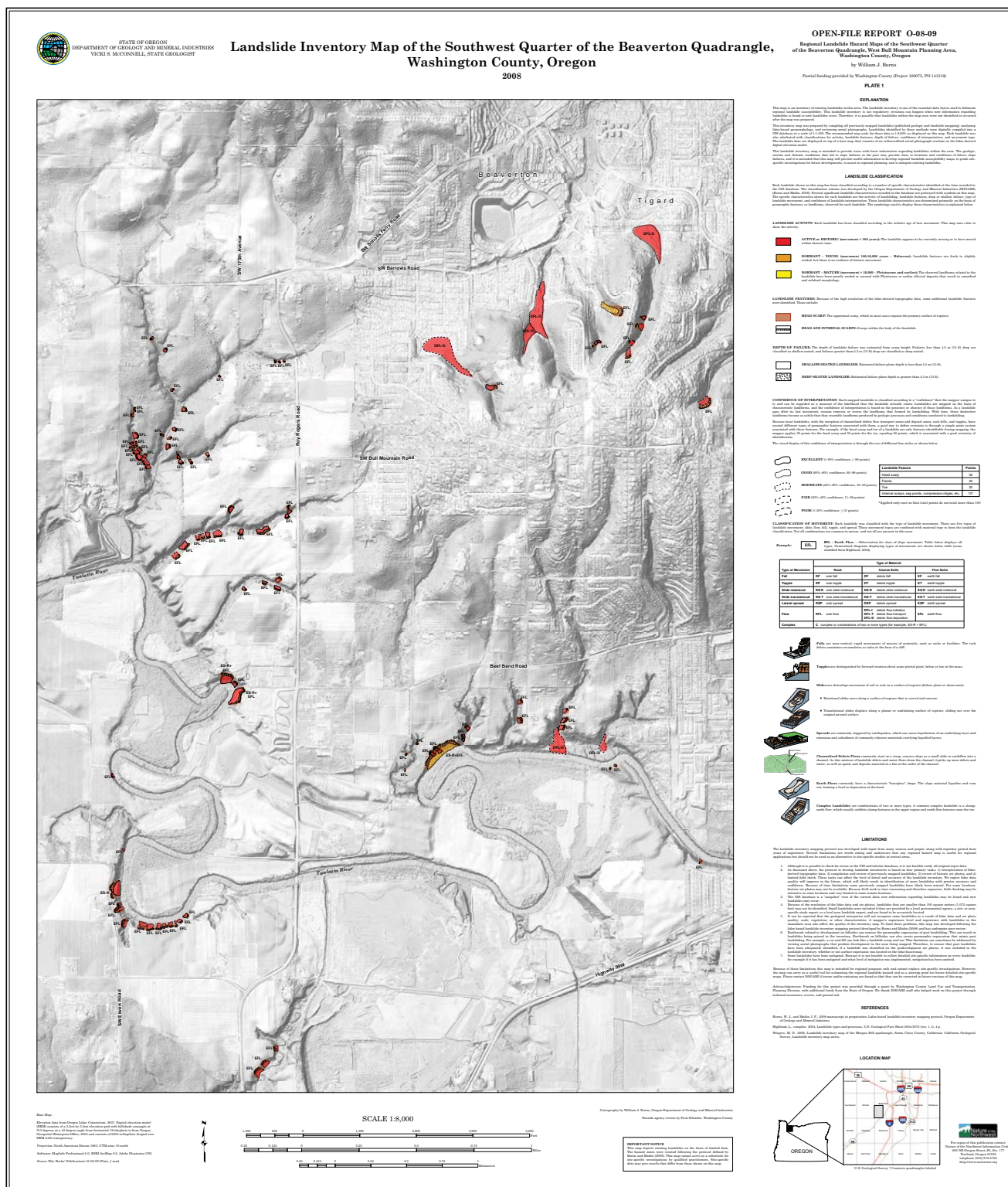


Figure 4. Landslide inventory map (facsimile of Plate 1 of this publication) of the southwest quarter of the Beaverton quadrangle, Washington County, Oregon.

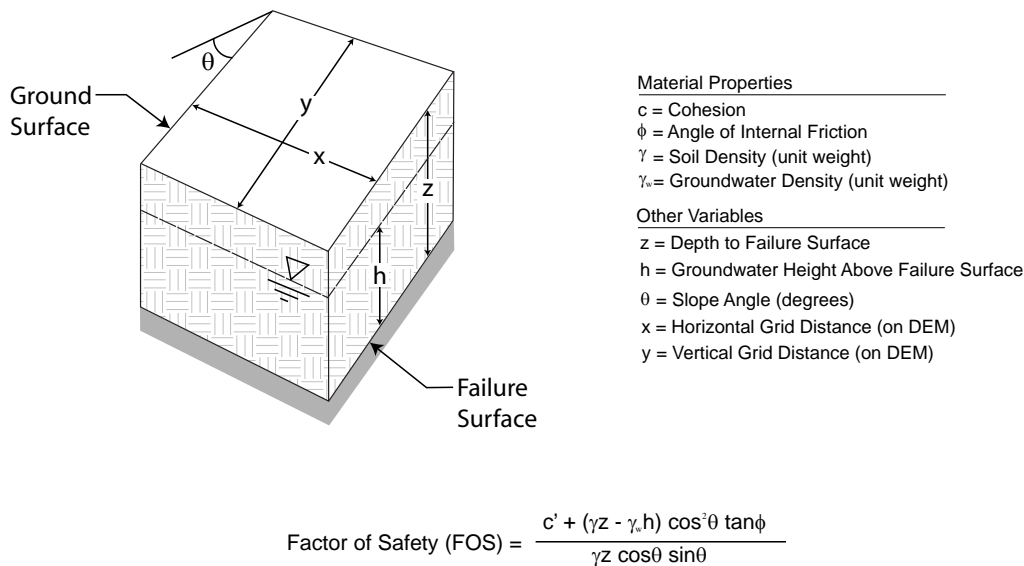


Figure 5. Infinite-slope analysis: diagram, parameters, and equation (Burns, 2008a; Cornforth, 2005).

Because the infinite slope equation for regional stability analysis is limited to a grid type analysis (i.e., the results are a calculated FOS for each individual grid, which does not consider the potential impact of adjacent slopes, etc.), we took a conservative approach in most steps to calculate the FOS. The limitations are discussed in greater detail later in this section and in Plate 2.

Several data sets are needed to calculate FOS throughout the area:

- geology — material properties
- depth to failure surface
- groundwater
- slope angle

Material properties consist of cohesion, angle of internal friction, soil density, and water density. Because these properties can vary from geologic unit to unit, we constructed a digital geologic map that contains the material properties for each unit (Figure 6). These properties can also vary within a particular geologic unit, so conservative values were used for each unit.

Because material properties are not readily available for the region, we constructed and used a set of conservative values (Table 2).

The maximum depth to failure surface, as defined by the cutoff between shallow- and deep-seated landslides, is 4.5 m (15 ft); however, the majority (mean) of shallow landslides in the region have a failure surface roughly 2.4 m (8 ft) deep. Thus a depth of 2.4 m (8 ft) was used in the infinite-slope equation (Figure 5).

The groundwater parameter can vary widely spatially and with time. Because of these potential variations, we selected a worst case scenario (most conservative) approach; complete saturation, or z , equals h (Figure 5).

The high-resolution lidar-derived digital elevation model (DEM) was used to create a map of slope angles for each grid cell (Figure 7) satisfying the slope angle parameter in the infinite slope equation.

Because there are many limitations to regional stability analysis using the infinite slope equation and unknowns due to general lack of material properties data spatially, we applied a 2:1 horizontal to vertical distance ratio (2H:1V; Figure 8) buffer to both the head scarp and the FOS, as described below.

Most landslides tend to leave a near-vertical head scarp above the failed mass. Commonly, this head scarp area will fail retrogressively or a separate landslide will form above the head scarp due to loss of resisting forces.

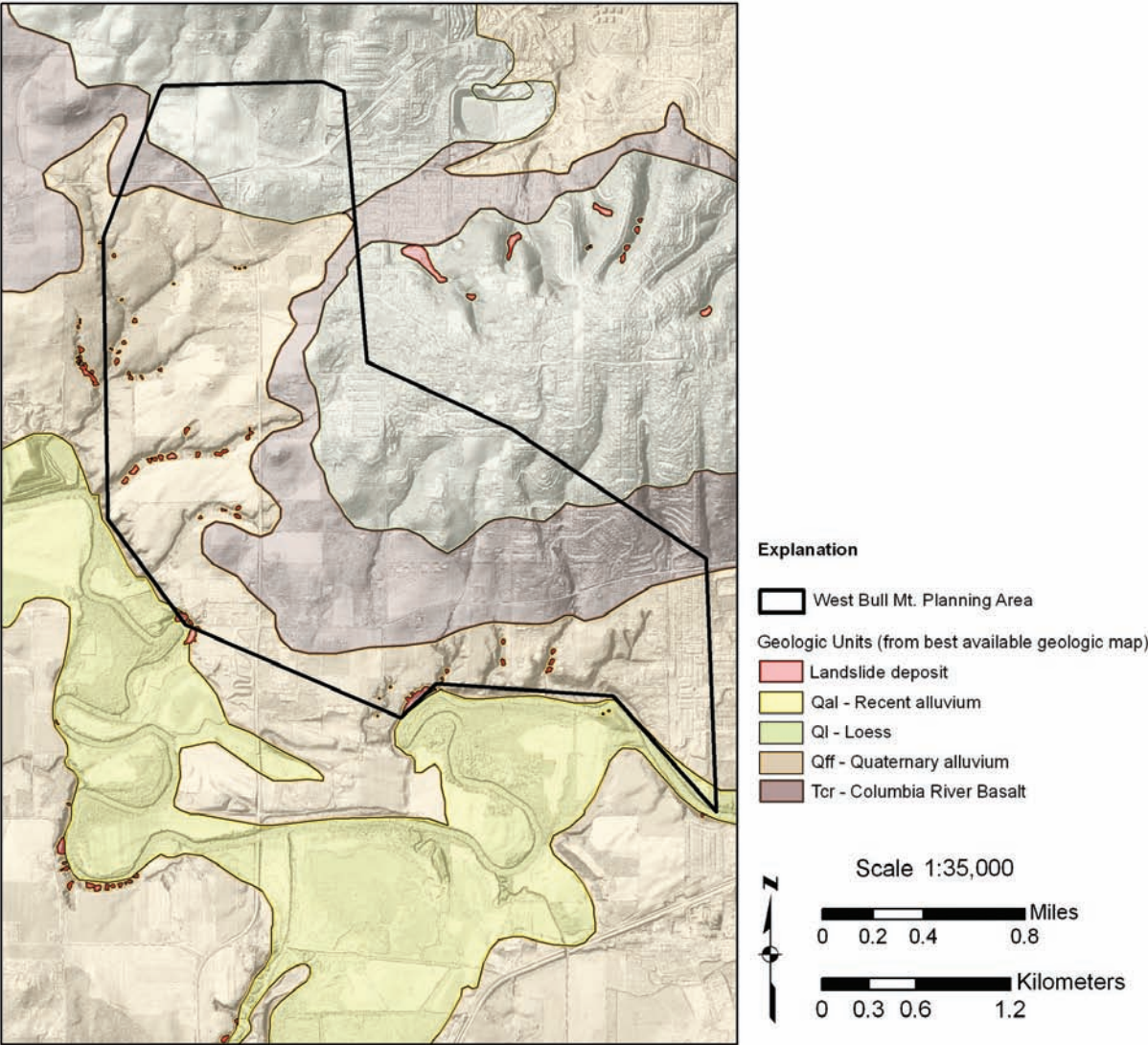


Figure 6. Geologic-material properties map of the southwest quarter of the Beaverton quadrangle, Washington County, Oregon (Madin, 2004, 1990).

Table 2. Conservative typical soil and rock material properties (Harp and others, 2006; Conforth, 2005; Denning, 1994).

	Common Lithology Description	Common Unit or Formation Names	Common Unit Label	Angle of Internal Friction (ϕ) (degrees)	Cohesion (c)		Unit Weight	
					(kPa)	(lb/ft ²)	(kN/m ³)	(lb/ft ³)
Cohesionless Soils								
Landslide deposit (deep failure)	shearing mainly along deep failure plane	Landslide	Qls	28	0	0	15.5	99
Recent alluvium (fine grained)	clay, silt, sand	Quaternary alluvium, loess	Qal, Qff, Ql	30	0	0	14.5	93
Cohesive Soils								
Residual soil on basalt/andesite	silty clay with boulders	Columbia River Basalt	Tcr	40	10	209	15	96
Water								
Water	water	water	W	0	0	0	10	64

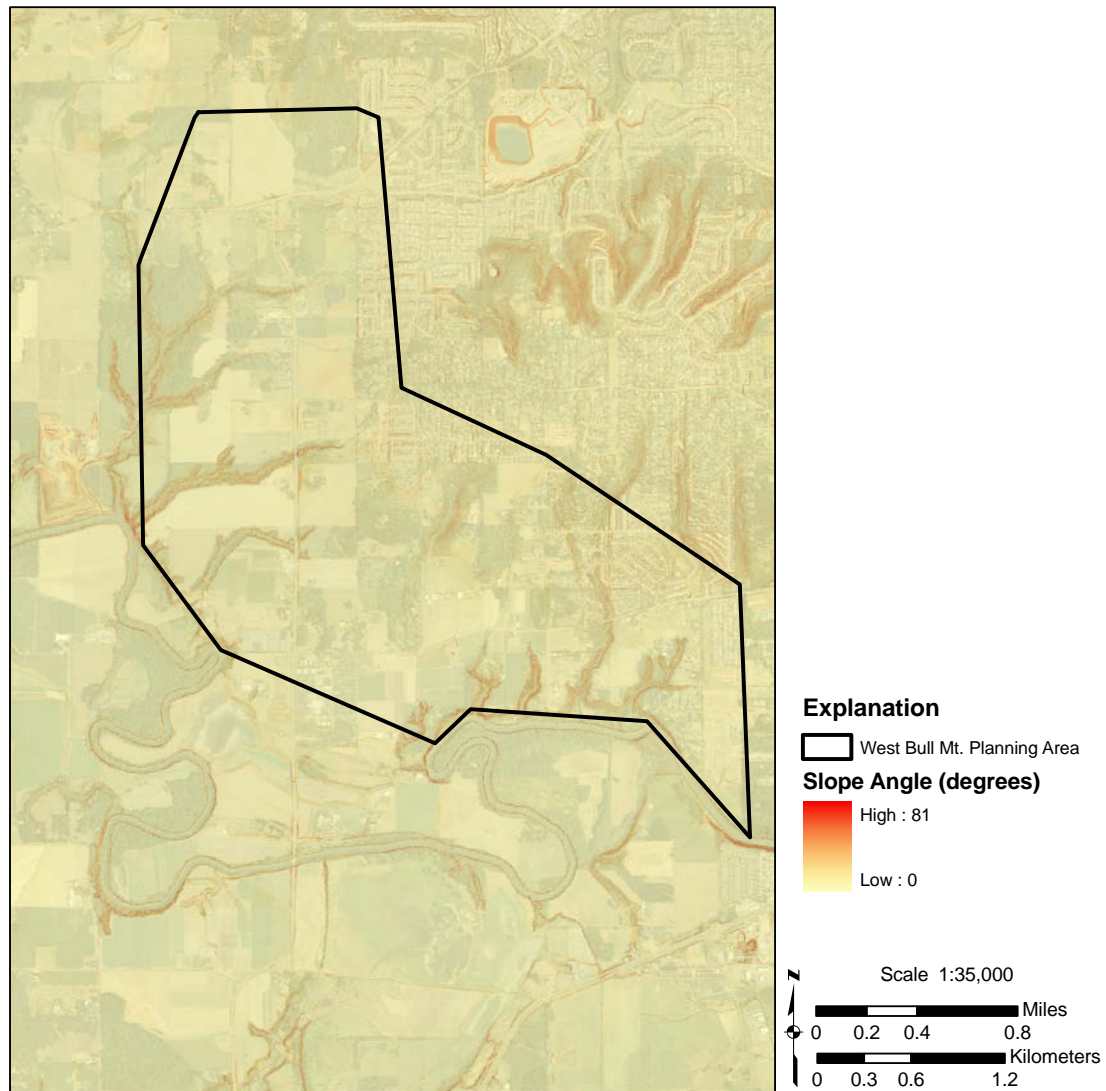


Figure 7. Slope map of the southwest quarter of the Beaverton quadrangle, Washington County, Oregon, created from lidar-derived digital elevation model.

Generally, the area above the head scarp has a relatively low slope angle; thus, the factor of safety calculated using the infinite-slope equation on a grid is relatively high — indicating a low susceptibility of future failure. To account for the increase in susceptibility of this area above the head scarp, which is missed when using the infinite-slope equation alone, we used a 2:1 horizontal to vertical distance ratio (2H:1V) head scarp buffer (Figure 9).

Because use of the infinite slope equation for regional stability analysis is limited to a grid type analysis (i.e., the results are a calculated FOS for each individual grid, which does not consider the potential impact of adjacent slopes, etc.), we applied a buffer to all areas with a calculated FOS less than 1.5 or the areas considered to be potentially unstable. This buffer was applied both up and down slope of the areas with a calculated FOS less than 1.5 as shown in Figure 10.

To create the final shallow-seated landslide hazard zones, we combined several of the contributing factors (Table 3).

To assist visualization, we created a 1:8,000-scale map (Plate 2; see facsimile in Figure 11) to display the lidar-based shallow-seated landslide susceptibility data (LSshallow-suscept.*; these GIS files are provided as part of this publication). We created the susceptibility zones following the protocol defined by Burns (2008a). This map cannot serve as a substitute for site-specific investigations by qualified practitioners. Site-specific data may give results that differ from those shown on this map. Several other limitations are listed on Plate 2.

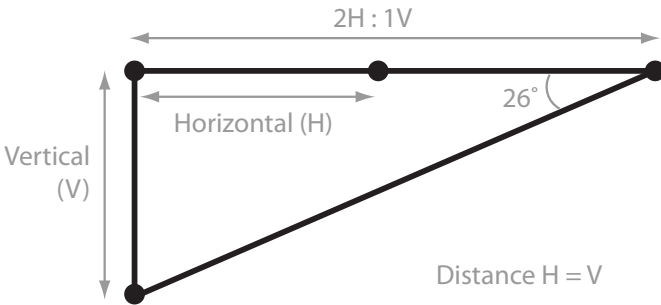


Figure 8. Diagram of the 2:1 horizontal to vertical distance ratio (2H:1V) used to create head scarp and factor of safety buffers.

Table 3. Final hazard zone matrix for shallow-seated landslides.

Contributing Factors	Final Hazard Zone		
	High	Moderate	Low
Factor of Safety (FOS)	less than 1.25	1.25 - 1.5	greater than 1.5
Landslide Deposits & Head Scarps	included	—	—
Buffers	2H:1V (head scarps)	2H:1V (FOS less than 1.5)	—

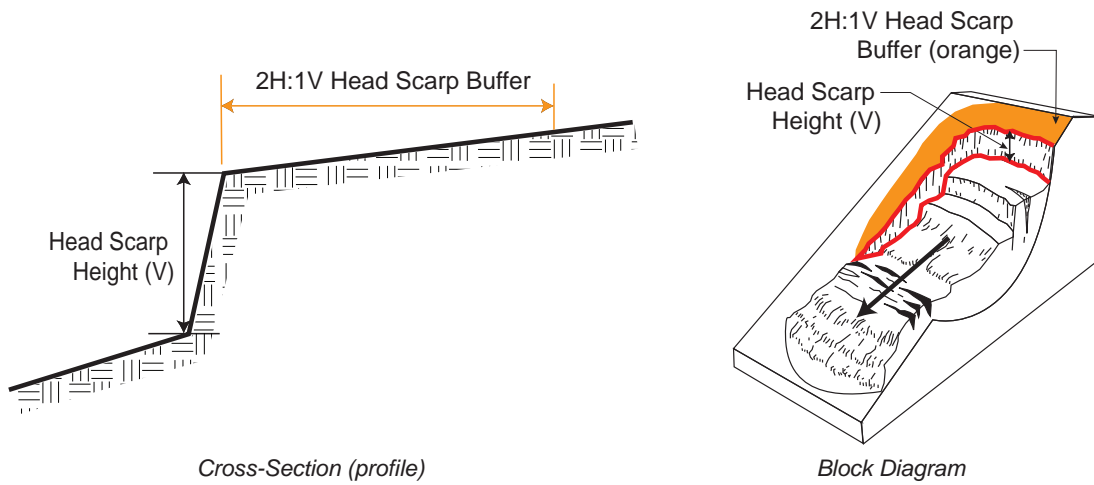


Figure 9. Diagram of the two horizontal to one vertical distance ratio (2H:1V) head scarp buffer.

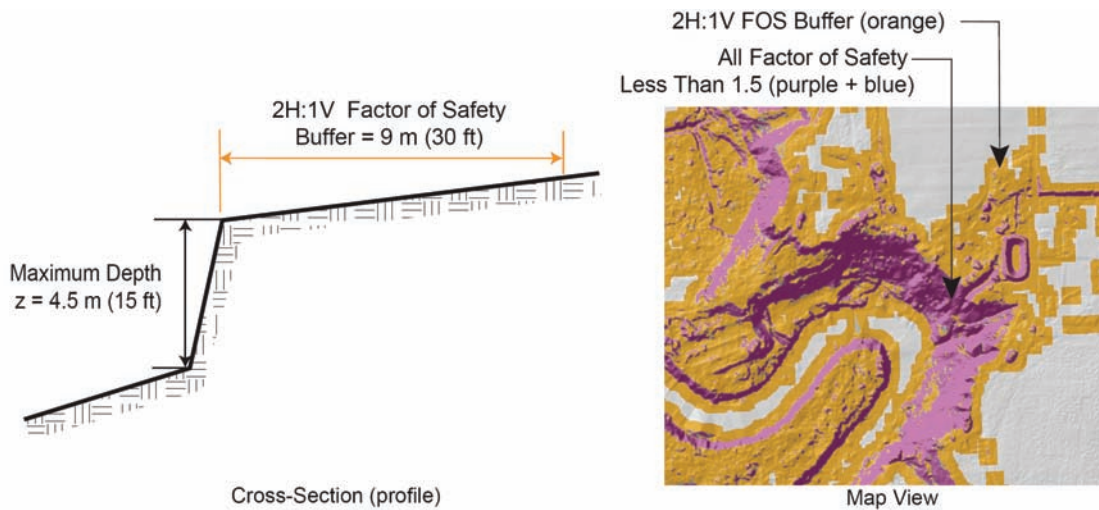


Figure 10. Diagram of the two horizontal to one vertical distance ratio (2H:1V) buffer applied to all factor of safety (FOS) less than 1.5.

4.3 Deep-seated landslide susceptibility

With the lidar-based landslide inventory and several other data sets, we created a deep-seated (depth greater than 15 ft [4.5 m]) susceptibility map using four main components (Burns, 2008b):

- deep-seated landslide inventory
- buffers
- geologic units and slope angles
- combination of the previous three factors into final susceptibility hazard zones

All deep-seated slides, flows, and spreads were queried out of the lidar-based landslide inventory database and saved to a separate GIS file.

Many deep-seated landslides move repeatedly over hundreds or thousands of years, and many times the continued movement is through retrogressive failure or progressive upslope failure of the head scarp. To account for this potential upslope hazard, we applied a buffer to all mapped deep-seated landslide deposits as shown in Figure 12.

Because there are many unknowns involved with regional susceptibility models, we also applied a 2H:1V buffer on all landslide head scarps as shown in Figure 13.

These two buffers were applied to all head scarps from the deep-seated landslide inventory. In all cases the greater of the two buffers was used.

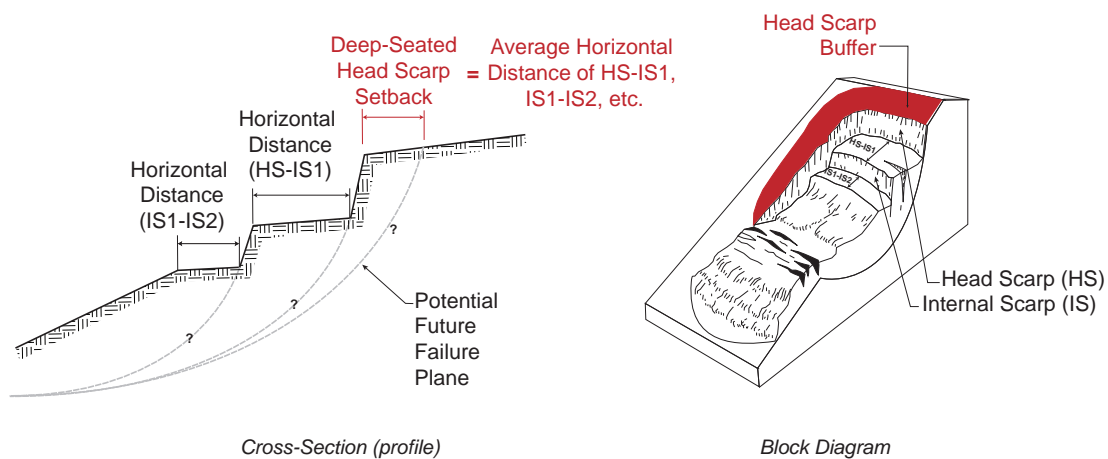


Figure 12. Head scarp retrogression buffer.

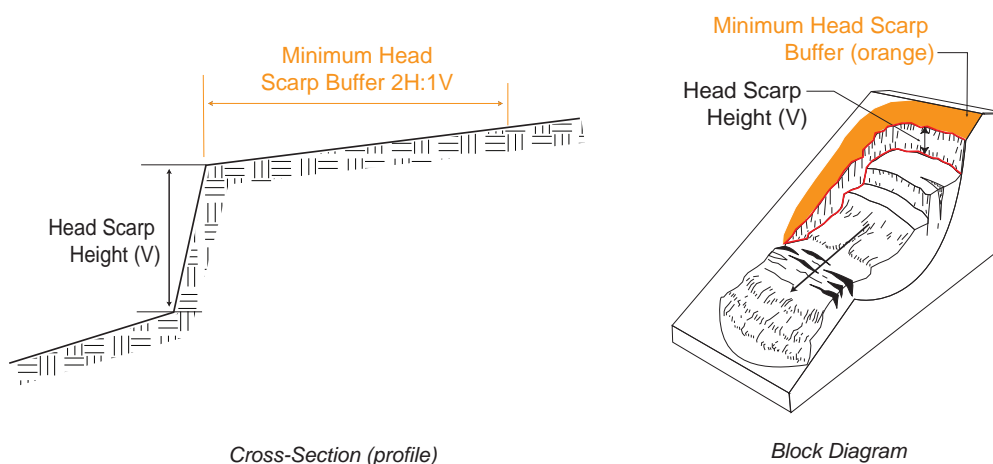


Figure 13. Head scarp buffer.

The last component in the deep-seated susceptibility model is a combination of four factors:

- susceptible geologic units or units that contain identified deep-seated landslides from the inventory
- slope angles greater than 10 degrees
- relative proximity to identified deep-seated landslides from the inventory
- educated judgment of the mapper

First, we set up a generalized geologic map overlain with slopes greater than 10 degrees (Figure 14). These two data sets, along with the other two factors (proximity and judgment), were used to create the boundary between the moderate and low deep-seated landslide susceptibility zones. A slope angle of 10 degrees was selected on the basis of the lowest measured slope in the landslide inventory database.

We followed the lidar-based deep-seated landslide susceptibility mapping protocol (Burns, 2008b) to create the moderate and low deep-seated susceptibility hazard zones. This map uses color to show different geologic units and slopes across the map.

To create the final deep-seated landslide hazard zones, we combined several of the contributing factors (Table 4).

The lidar-based deep-seated landslide susceptibility data (LSdeep-suscept.shp; these GIS files are provided as part of this publication) are presented on a 1:8,000-scale map (Plate 3; see facsimile in Figure 15). The susceptibility zones were created following the protocol defined by Burns (2008b). This map cannot serve as a substitute for site-specific investigations by qualified practitioners. Site-specific data may give results that differ from those shown on this map. Several other limitations are listed on Plate 3.

5.0 RESULTS AND DISCUSSION

We used a lidar-based landslide inventory mapping protocol (Burns and Madin, 2008) to create a landslide inventory of the southwest quarter of the Beaverton, Oregon, topographic quadrangle. Ninety-eight landslide deposits were located. Forty-seven of these are within the WBMPA. Eighty-three of these were classified as shallow, nine as deep, and six as debris flow deposits. The average prefailure slope angle is 28 degrees. The average landslide area is roughly 20,000 ft² (1850 m²), which is approximately the size of a football field. The average depth of failure for the shallow-

seated landslides is 8.5 ft (2.6 m), and the average depth of failure for the deep-seated landslides is 26 ft (7.9 m).

We used a lidar-based shallow-seated landslide susceptibility mapping protocol (Burns, 2008a) to create a shallow-seated landslide susceptibility map of the southwest quarter of the Beaverton quadrangle. The area of the southwest quarter of the quadrangle is roughly 13 mi² (37 km²); 2.0 mi² (5.2 km²) of the total are classified as highly susceptible to shallow-seated landslides, 6.5 mi² (16.3 km²) as moderately susceptible to shallow-seated landslides, and 4.7 mi² (12.2 km²) as less susceptible to shallow-seated landslides.

We used a lidar-based deep-seated landslide susceptibility mapping protocol (Burns, 2008b) to create a deep-seated landslide susceptibility map of the southwest quarter of the Beaverton quadrangle. The area of the southwest quarter of the quadrangle is roughly 13 square miles; 0.03 square miles of the total 13 are classified as highly susceptible, 2.5 square miles as moderately susceptible, and 10.5 square miles as less susceptible to deep-seated landslides.

As previously discussed, we developed the landslide inventory and shallow-seated susceptibility maps with input from many sources and expertise gained from years of experience; however, several limitations underscore that these maps are designed for regional applications and should not be used as an alternative to site-specific studies in critical areas. These limitations are described in detail on Plates 1–3.

Note about the base map on the map plates.

The base map I developed for the map plates is an unusual approach. Because others may want to use this technique, I include a short description of how I developed it.

The base consists of two layers: a hillshade image and an aerial photograph image. I created the hillshade image by transforming the original digital elevation model (DEM) using the “hillshade” tool in the Spatial Analysis Extension of ArcGIS 9.2. The DEM was first multiplied by 5 times (vertical exaggeration) prior to the hillshade image creation to enhance slope areas. The settings in the “hillshade” tool include a sun angle at 315 degrees and at 45 degrees from the horizontal. I applied a transparency of 40% to this layer.

I used 2005 statewide orthorectified images to create the aerial photo layer. I changed the images from an RGB composite (multi-color) to a stretched color ramp from white to black (i.e., grayscale). Again, I applied a transparency of 45% to this layer.

Finally, I grouped the two layers with the hillshade image on top of the orthophoto image and applied a brightness of 20%.

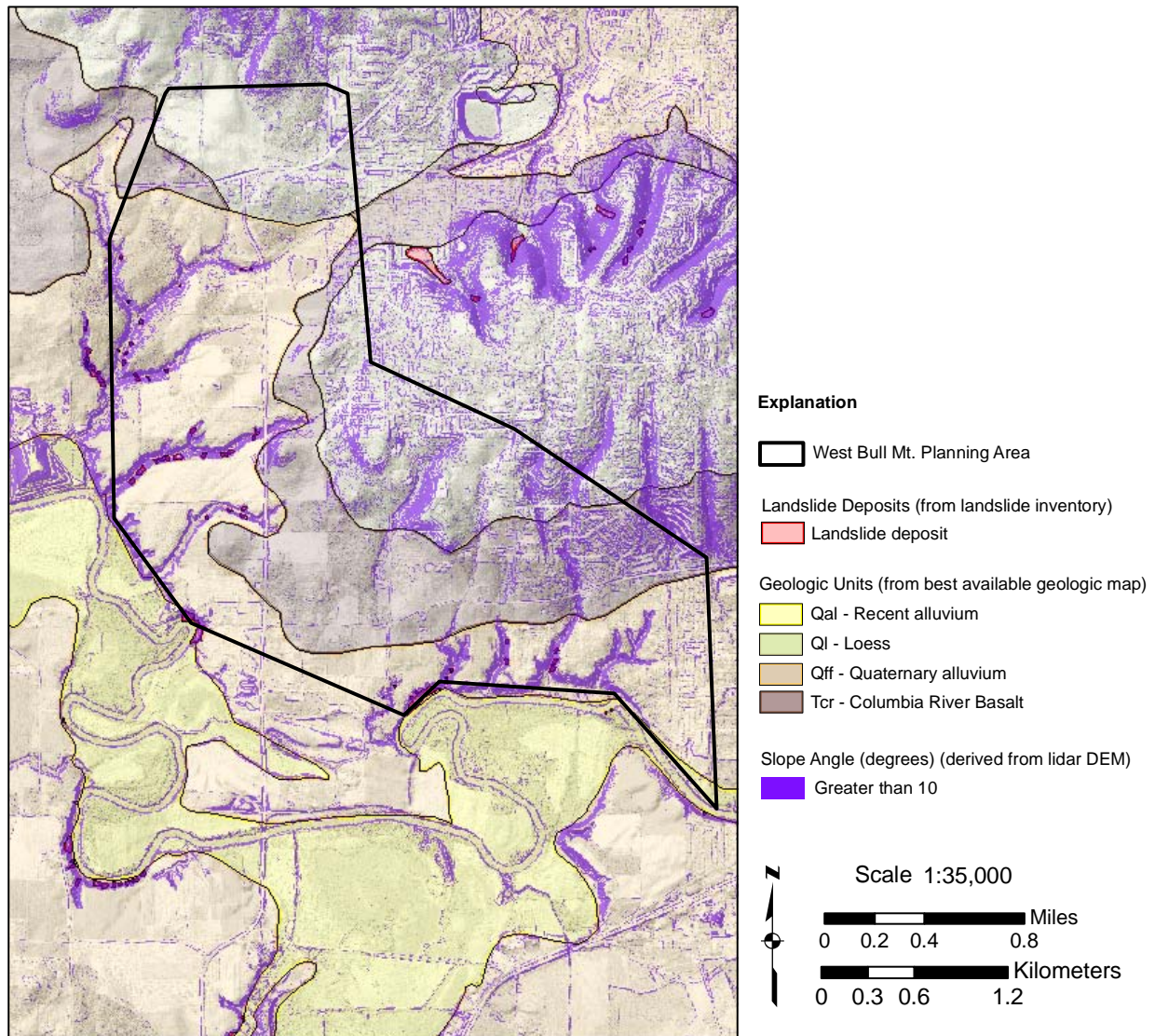


Figure 14. Generalized geologic map of the southwest quarter of the Beaverton quadrangle, Washington County, Oregon, overlain with slopes greater than 10 degrees and identified deep-seated landslides.

Table 4. Final hazard zone matrix for deep-seated landslides.

Contributing Factors	Final Hazard Zone		
	High	Moderate	Low
Landslide Inventory	included	—	—
Head Scarp Buffers	included	—	—
Additional Factors	—	included	included

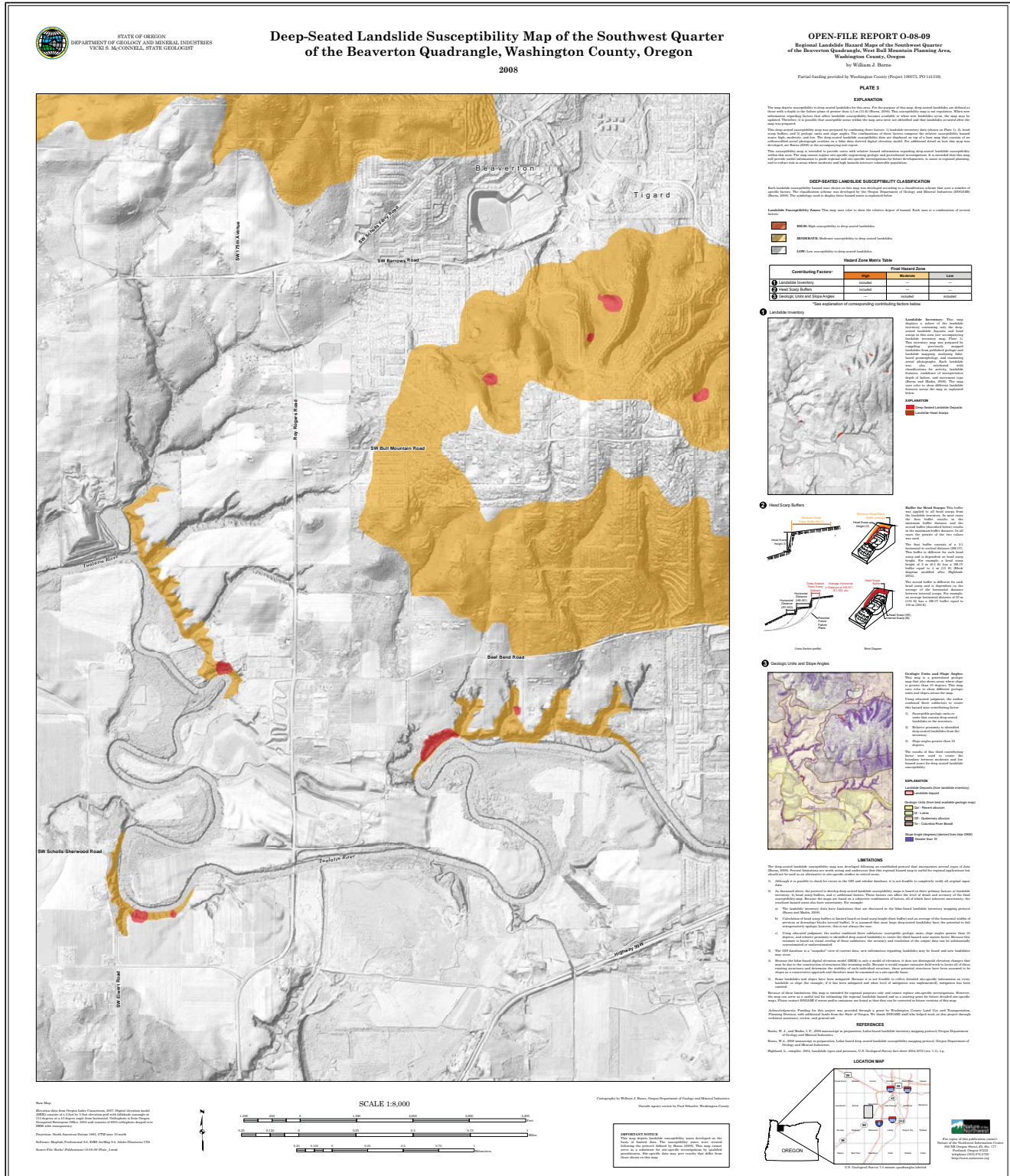


Figure 15. Deep-seated landslide susceptibility map (facsimile of Plate 3 of this report) of the southwest quarter of the Beaverton quadrangle, Washington County, Oregon.

6.0 RECOMMENDATIONS

These maps are intended to provide users with basic information regarding landslides and susceptibility to shallow-seated landslides within the mapped area. The maps contain useful information to guide site-specific investigations for future development, to assist in regional planning and development, to mitigate existing landslides and slopes, and to prepare for emergency situations, such as storm events and earthquakes.

We reiterate that this database is not appropriate for site-specific evaluations, but it is valuable for regional screening for landslides and selection of appropriate areas on which to focus site-specific studies. The database is particularly suitable for incorporation and into regional GIS databases for a multitude of purposes. These include but are not limited to city and county hillside development ordinances, issuance of building permit conditions, public works planning and operations, and environmental and sustainability issues.

7.0 ACKNOWLEDGEMENTS

Funding was provided by the Washington County Land Use and Transportation Department, Planning Division (intergovernmental agreement with Washington County, project 100075, purchase order 141319), with additional funds from the State of Oregon. I thank DOGAMI staff who helped with this project through technical assistance, review, and general aid, especially Yumei Wang, Ian Madin, and Deb Schueller.

8.0 REFERENCES

- Burns, W. J., 1999, Engineering geology and relative stability of the southern half of Newell Creek canyon, Oregon City, Oregon: Portland State University, Department of Geology, M.S. thesis, 143 p., 3 plates.
- Burns, W. J., 2008a, Lidar-based shallow-seated landslide susceptibility mapping protocol: Oregon Department of Geology and Mineral Industries, in preparation.
- Burns, W. J., 2008b, Lidar-based deep-seated landslide susceptibility mapping protocol: Oregon Department of Geology and Mineral Industries, in preparation.
- Burns, W. J., and Madin, I. P., 2008, Lidar-based landslide inventory mapping protocol: Oregon Department of Geology and Mineral Industries, in preparation.
- Burns, S. F., Burns, W. J., James, D. H., and Hinkle, J. C., 1998, Landslides in the Portland, Oregon, metropolitan area resulting from the storm of February 1996: Inventory map, database, and evaluation: Portland State University, Department of Geology, report to Metro, contract 905828, 68 p.
- Burns, W. J., Madin, I. P., and Ma, L., 2008, State-wide landslide information database for Oregon (SLIDO), release 1. [Web: <http://www.oregongeology.org/slido/>]
- Cornforth, D. H., 2005, Landslides in practice: Investigation, analysis, and remedial/preventative options in soils: Hoboken, N.J., John Wiley and Sons, Inc., 596 p.
- Denning, C., 1994, Fundamental stress-strain relationships, in Hall, D. E., Long, M. T., and Remboldt, M. D. eds., Slope stability reference guide for National Forests in the United States, Forest Service Publication EM-7170-13: Washington, D. C., United States Department of Agriculture, v. II, p. 331–343.
- Harp, E. L., Michael, J. A., and Laprade, W. T., 2006, Shallow-landslide hazard map of Seattle, Washington, U.S. Geological Survey Open-File Report 2006-1139, 20 p.
- Hofmeister, R. J., 2000, Slope failures in Oregon: GIS inventory for three 1996/97 storm events: Oregon Department of Geology and Mineral Industries Special Paper 34, 20 p.
- Hofmeister, R. J., Miller, D. J., Mills, K. A., Hinkle, J. C., and Beier, A. E., 2002, GIS overview map of potential rapidly moving landslide hazards in western Oregon: Oregon Department of Geology and Mineral Industries Interpretive Map Series IMS-22, 52 p.
- Madin, I. P., 1990, Earthquake hazard geology maps of the Portland metro area, Oregon Department of Geology and Mineral Industries Open-File Report O-90-02.
- Madin, I. P., 2004, Geologic mapping and database for Portland area fault studies: Final report, Clackamas, Multnomah, and Washington Counties, Oregon: Oregon Department of Geology and Mineral Industries Open-File Report O-04-02.
- Sidle, R. C., and Ochiai, H., 2006, Landslides: processes, prediction, and lands use, Water Resources Monograph 18: Washington, D.C., American Geophysical Union, 312 p.